Research Article Vol. 6, No. 3 / March 2019 / Optica 304

Soliton self-mode conversion: revisiting Raman scattering of ultrashort pulses

L. Rishøj,[1] B. Tai,[1] P. Kristensen,[2] and S. Ramachandran[1,*]

[1]Boston University, 8 St. Mary's St, Boston, Massachusetts 02215, USA
[2]OFS-Fitel, Priorparken 680, Brøndby 2605, Denmark
*Corresponding author: sidr@bu.edu

Received 26 October 2018; revised 25 January 2019; accepted 13 February 2019 (Doc. ID 349344); published 5 March 2019

Coherent frequency conversion in compact integrated formats via guided-wave nonlinear optics has not been shown to be power scalable to date, because single-mode waveguides need dispersion control, achieved by shrinking mode size and hence reducing power-handling capacity, whereas power-tolerant multimode waveguides yield spatially incoherent, hence uncontrollable, nonlinear coupling. Here we report the discovery of a new manifestation of Raman scattering of ultrashort pulses that is power scalable while yielding pure spatially coherent beams. The phenomenon of soliton self-mode conversion (SSMC) described in this paper exploits the group-velocity diversity of multimode waveguides, enabling noise-initiated Raman scattering of an ultrashort pulse to occur exclusively between two distinct spatial eigenmodes and only those two modes. This exclusivity helps in naturally maintaining spatial coherence, which is usually the bane of multimode waveguide nonlinear optics. And, the fact that this phenomenon occurs in mode-size-scalable multimode waveguides yields the power scalability. SSMC is wavelength agnostic, since it can occur at virtually any wavelength in which a multimode fiber is transparent, and we demonstrate its versatility by frequency-converting a conventional 1-μm fiber laser into MW-peak power, ∼75-fs pulses at the biologically crucial 1300-nm spectral range. This represents an enhancement, by roughly two orders of magnitude, of nonlinear frequency-converted power levels of ultrashort pulses at 1300 nm directly out of any flexible fiber, to date.

https://doi.org/10.1364/OPTICA.6.000304

1. INTRODUCTION

Raman scattering has long been a powerful means to obtain frequency-converted source generation in guided wave media, since optical guidance provides the long interaction lengths over which the relatively weak nonlinear scattering mechanism can build up. At its most fundamental level, an optical pump wave provides peak gain to light at a frequency that is down-shifted by one Stokes shift, related to the energy of the optical phonon that is emitted. Stimulated Raman scattering (SRS) is the name given to a manifestation of this process when the pump wave initially interacts with noise photons at the Stokes frequency, which then get sufficiently amplified via Raman scattering to act as a strong enough seed to grow rapidly at the expense of the original pump. The Stokes shift is typically large—as much as 13 THz in silica, often more in biological molecules. However, SRS of this form is not known to occur for ultrashort pulses. This is because group-velocity dispersion (GVD) of the medium along with this large Stokes shift implies that the group velocity of pulses at the pump and Stokes frequencies is different enough that, for short enough pulse widths, the pulses may completely walk off. In fact, this effect is so severe that for pulses shorter than a few picoseconds, discrete, noise-initiated SRS cannot occur at all. Instead, ultrashort pulses experience a distinct, incremental, continuous wavelength shift, since the broad bandwidth of an ultrashort pulse enables the blue spectral portion of the pulse to act as a Raman "pump" for the red portion of its own spectrum. This effect, coined soliton self-frequency shift (SSFS) by Mitschke and Mollenauer [1] upon its discovery in 1986, is a self-seeded process and the primary Raman scattering mechanism known for ultrashort pulses. In general, "self-action" manifestations of Raman scattering in optical fibers and waveguides can be categorized within these two broad classes—SRS for CW and quasi-CW (long) pulses [2–5], and SSFS for ultrashort pulses [6–11]. Given the key role played by group velocity and associated pulse walk-off in determining the very nature of the manifestation of Raman scattering (noise-initiated or self-seeded, discrete or CW shift, partial or full conversion, etc.), unexpected behavior may occur in the emerging field of multimode optics, of interest for diverse applications including super-resolution microscopy [12] and information capacity scaling [13], because multimode fibers provide a plethora of group-velocity tailoring possibilities arising from their high modal dimensionality.

Here, we report the discovery of a unique nonlinear Raman coupling phenomenon, distinct from the aforementioned well-known SRS and SSFS, with no direct analog in bulk or guided wave systems. Given the large density of states in a multimode fiber, two distinct spatial modes, and only those two modes,

may have identical group velocities at specific spectral separations. When this spectral separation corresponds to the frequency difference at which nonlinear Raman gain is maximized, efficient coupling between the modes may be expected, and a spectrally separated new ultrashort pulse in a different mode initiates from quantum noise [14]. However, owing to the strong coupling *and* exclusive group-velocity selectivity, this results in the transfer of ∼100% of the photons from the original pulse to this new pulse [15]. Raman gain mediated by group-velocity matching between modes has been observed in birefringent fibers and ring resonators before, but only when both interacting pulses were seeded [16,17] or when a resonant cavity was employed [18]. We observe this Raman effect, called soliton-self mode conversion (SSMC) henceforth, in fibers with mode counts exceeding 10,000. The system self-selects precisely one nonlinear process out of the multitude of possibilities, without the need for seeding with extraneous waves, employing spatial or spectral filters, or operating in a resonant cavity. Nevertheless, despite the fact that SSMC is a spontaneous process, originating from quantum noise, it still dominates the concurring self-seeded process of SSFS, which points to an interesting phenomenon where a noise-initiated process wins over a concurrent seeded process. Using SSMC, we demonstrate ∼600-nm-wide wavelength translations (limited only by available pump power), as well as the ability to obtain record peak powers of 1.1 MW (80 nJ, 74 fs) at the biologically crucial ∼1300-nm spectral range.

2. OBSERVATION OF SSMC

Consider a soliton pulse, with ∼17-nm spectral bandwidth at ∼1120 nm, in the $LP_{0,21}$ mode [measured mode image in Fig. 1(c)] at the input of a step-index silica multimode fiber with 0.34 numerical aperture (NA) and 97-μm core diameter. The schematic of the experimental setup is shown in Fig. 1(b). The desired mode is excited in the fiber by encoding the spatial phase onto a Gaussian beam using a spatial light modulator (SLM); more details about the experimental setup, fiber characteristics, and the mode excitation method are provided in Supplement 1. This fiber supports ∼10,735 spatial eigenmodes, but since the $LP_{0,m}$ modes are increasingly more linearly stable to bend perturbations as the radial order m increases [19], and they also possess anomalous GVD [20], a pulse in this mode is expected to behave like any soliton and experience frequency shifts due to SSFS as input power or fiber length increases [21,22]. Here, a rather unexpected phenomenon occurs—Fig. 1(e) shows the spectra at the output of the fiber measured for increasingly higher launched pump pulse energies. The soliton does indeed appear to shift its frequency by the conventional SSFS effect, but starts losing energy to a new spectral feature, spontaneously formed at a spectral separation of ∼15 THz. For sufficient input power, complete conversion of the photons in the original pulse to this new pulse occurs. Imaging the output of the fiber with appropriate spectral filters reveals that this spectral feature is in a different spatial eigenmode, the $LP_{0,20}$ mode [Fig. 1(d)], which is exactly one radial order lower than the input mode. We systematically imaged all the spectral features in the red and green wavelength windows, and confirmed that they correspond to the $LP_{0,21}$ and $LP_{0,20}$ modes, respectively. Figure 1(f) shows that the group index at 1140 nm of the input $LP_{0,21}$ mode is identical to that of the $LP_{0,20}$ mode at 1210 nm, and this frequency separation is close to the peak of the Raman gain coefficient—i.e., one Raman Stokes shift away. Thus, SSMC represents the complete conversion of an ultrashort pulse in one mode into an ultrashort pulse in another mode, when the spectral separation of two group-velocity-matched modes is close to maximum Raman gain. For a step-index fiber, the generated pulse is typically in a lower mode order, since the group index increases with increasing mode order for a fixed wavelength, and the group index for a given mode increase with wavelength [Fig. 1(f)] for well-guided modes. Note that this process [schematically illustrated as a function of fiber length in Fig. 1(a)] wins over conventional SSFS, although

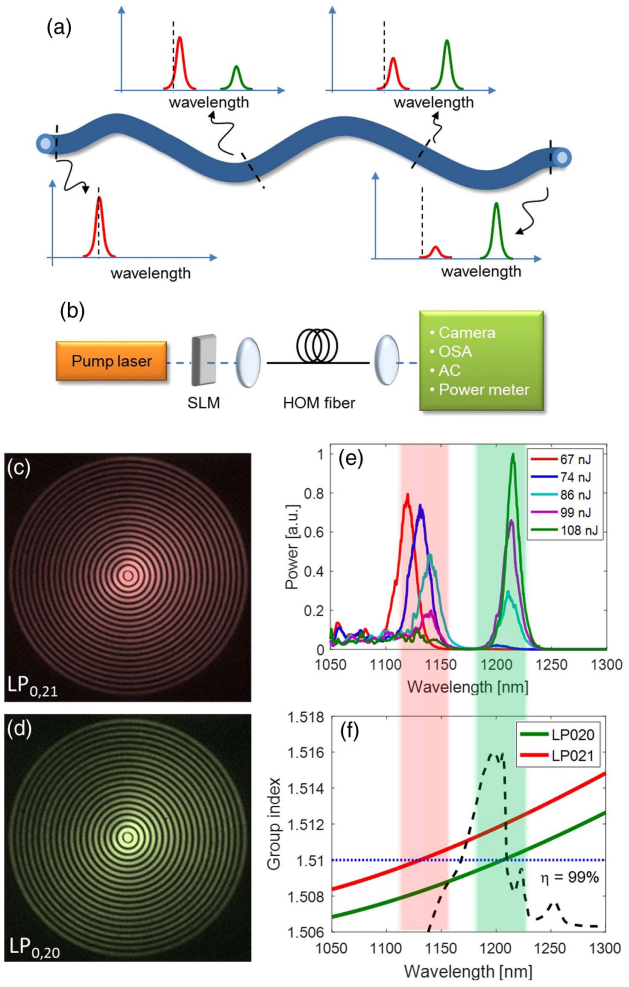

Fig. 1. (a) Schematic illustration of pulse evolution along a fiber via soliton self-mode conversion (SSMC). The red and green colored pulses denote different spatial modes, and the dashed black line marks the center wavelength of the input pulse. As the input soliton pulse (red) propagates along the fiber, it generates a new pulse (green) via Raman scattering in a different spatial mode that is group-index matched to the original pulse. Further propagation completely depletes the original pulse, resulting in transfer of power from one mode to another via this self-organized nonlinearity. (b) Schematic of the experimental setup. (c) Experimental image of the $LP_{0,21}$ mode and (d) $LP_{0,20}$ mode. (e) Experiment demonstrating the SSMC process. Energy transfer occurs between two group-index-matched modes, the spectral components in the red and green shaded boxes are in the $LP_{0,21}$ and $LP_{0,20}$ modes, respectively. (f) Group index as a function of wavelength for the two modes; black dashed line indicates the Raman gain coefficient. This illustrates that SSMC is the preferred nonlinear phenomenon when group-index-matched spectral separation matches with the Stokes shift of Raman scattering.

the latter is a self-seeded process typically expected to dominate noise-initiated nonlinear coupling phenomena.

This competition between SSMC and conventional SSFS is captured well by measuring the full pulse evolution in a similar step-index fiber (NA ~ 0.34; core-diameter ~87 μm) [23]. For this experiment a 100-fs pulse with 72.4-nJ energy at 1045 nm (KMLabs, Y-Fi) is used to excite an $LP_{0,19}$ mode at the fiber input. Figure 2(a) shows the spectral evolution with propagation length obtained via cutback of the original 12-m-long fiber, while the fiber launch condition was unchanged, along with measured mode images [Figs. 2(b)–2(f)]. Initially, a soliton formed in the $LP_{0,19}$ mode red-shifts via conventional SSFS to 1141 nm after 33 cm of propagation. At this point, it is group-index matched to the $LP_{0,18}$ mode at 16-THz frequency separation (i.e., within the Raman gain bandwidth). Hence, power transfer from the $LP_{0,19}$ pulse to the vastly wavelength-separated $LP_{0,18}$ mode commences, and after ~40 cm of propagation, the mode and wavelength conversion is complete. Thereafter, the new fundamental soliton in the $LP_{0,18}$ mode shifts to 1257 nm via conventional SSFS, when it becomes group-index matched to the $LP_{0,17}$ mode at 14-THz frequency separation. As in the previous case, with further propagation, full power transfer to the $LP_{0,17}$ mode is achieved via SSMC. These alternating intra-modal (SSFS) and intermodal (SSMC) processes repeat along the fiber—at the longest tested fiber length, a pulse at 1587 nm in a pure $LP_{0,15}$ mode is obtained. All modes are observed at wavelengths at least 360 nm below their respective cutoff wavelengths, and are thus all well guided in the fiber. Analysis of the spectral and temporal bandwidths of the pulses (Fig. S2 in Supplement 1) reveals 100% photon conservation—i.e., complete transfer of optical power—across each of these SSMC steps. Autocorrelation measurements were carried out for the pulse after 7 m in the $LP_{0,16}$ mode and the pulse after 12 m in the $LP_{0,15}$ mode; based on calculated time-bandwidth products, these pulses were found to be transform limited.

3. PULSE CHARACTERIZATION AND POWER SCALING

It is clear from the results illustrated in Figs. 1 and 2 that the SSMC phenomenon affects complete, frequency, and modal conversion either as the propagation length or pump power is increased. Figure 3 describes measurements from an arrangement that enables achieving record peak power levels of frequency-converted emission at the biologically crucial 1300-nm spectral range. A 1030-nm pump laser emitting 370-fs pulses excites an $LP_{0,21}$ mode in a 54-cm-long 97-μm-core-diameter fiber with NA ~ 0.34. For relative input pump powers <4 dB, conventional SSFS in the $LP_{0,21}$ mode yields a pulse-energy-versus-pump-power slope of 5.6 nJ/dB [Fig. 3(a)], and the pulse eventually reaches 1207 nm. Between relative pump power levels ~4.5–5.5 dB, a SSMC process occurs generating a pulse in the $LP_{0,20}$ mode at a slope efficiency of ~92.3 nJ/dB. This dramatically higher slope clearly illustrates that the quantum-noise initiated process of SSMC dominates the conventional self-seeded process of SSFS [14]. Once full conversion transpires, the SSMC-generated pulse undergoes traditional SSFS again, as evident from an energy-versus-pump-power slope (6.2 nJ/dB) similar to that of the original soliton. Autocorrelation traces of the lower wavelength pulse in the $LP_{0,21}$ mode prior to the initiation of SSMC reveal pulse durations of ~60 fs, whereas the longer wavelength pulses in the $LP_{0,20}$ mode during and after SSMC are ~74–78 fs wide [24]. The different pulse widths of the soliton before and after SSMC are consistent with the fact that the fiber parameters (GVD of the mode D, mode area A_{eff}—see Supplement 1, Fig. S1) are different for the different modes and wavelengths, and the need for a photon-conserving process to maintain soliton number N, given by $N^2 = 4\pi^2 c n_2 P T_0^2 / D\lambda^3 A_{\text{eff}}$, where n_2 is the nonlinear coefficient, P is the power, and T_0 is the pulse duration. Figure 3(b) shows that the normalized soliton number for the SSFS soliton is nominally constant, as expected. However, the SSMC-generated pulse, while always

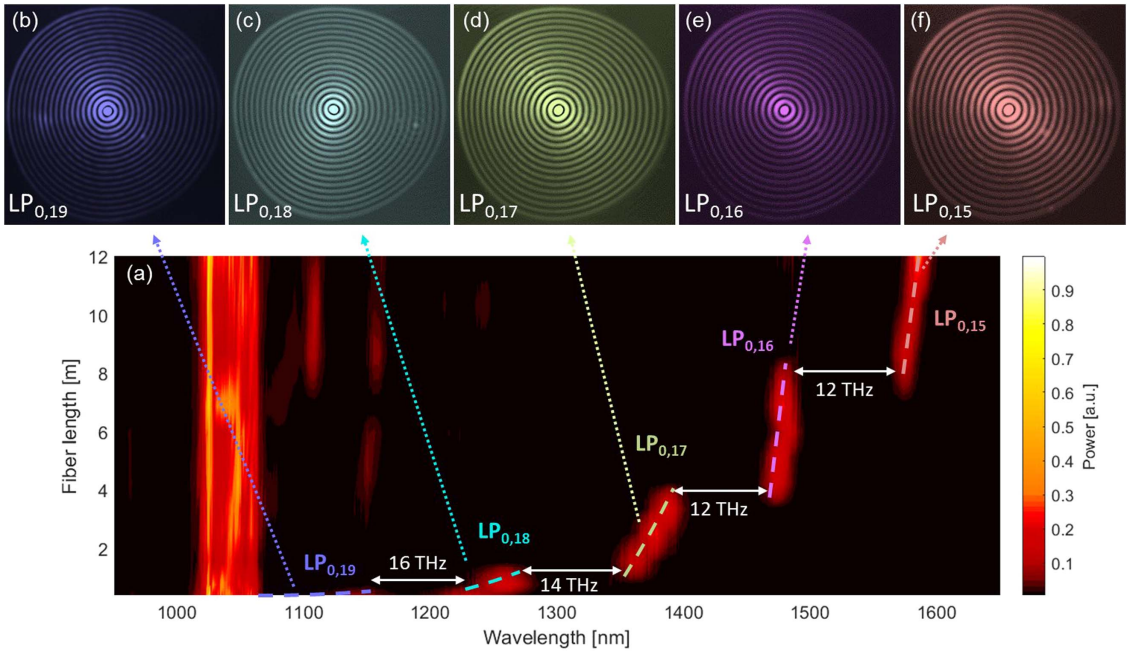

Fig. 2. (a) Spectra as a function of fiber length; the launched pulse at 1045 nm is in the $LP_{0,19}$ mode. (b)–(f) Representative mode images taken using 10-nm bandpass filters of various spectral features.

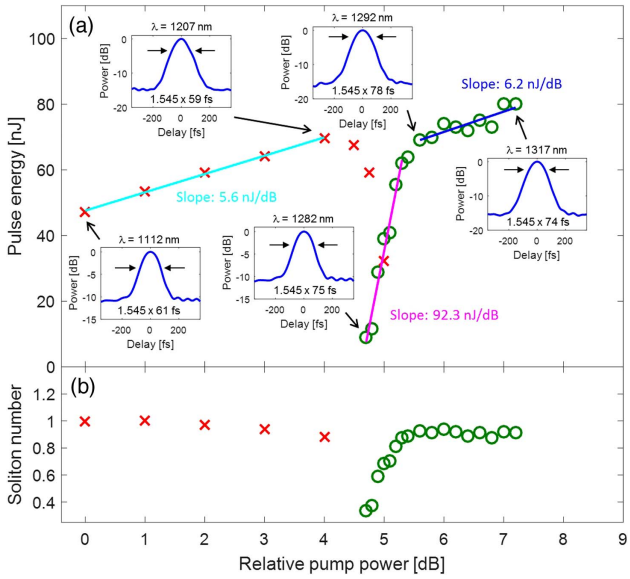

Fig. 3. (a) Pulse energies for the pulse in the $LP_{0,21}$ mode (red crosses) and the SSMC pulse in the $LP_{0,20}$ mode (green circles) as a function of relative pump power. Linear fits to the various slopes are provided on the plot. The insets are autocorrelation data for four selected pulses. (b) Soliton number normalized with respect to the pulse at the lowest pump power.

transform limited (verified via time-bandwidth product calculations based on spectral width and autocorrelation measurements) regardless of its energy, initially has a normalized soliton number of only 0.3 before rapidly approaching unity. This indicates that the SSMC pulse is not a traditional soliton, and instead, a combination of intermodal cross-phase modulation and Raman gain serves to preserve its pulse width. Note that whenever the conditions for SSMC are met, either for the single transition depicted in Fig. 1, or the multiple SSMC transitions shown in Fig. 2, full conversion occurs, and photon number is conserved. Hence, when the intermodal group-velocity-matching condition is satisfied, SSMC is the preferred nonlinearity over the self-seeded, conventional SSFS process [25].

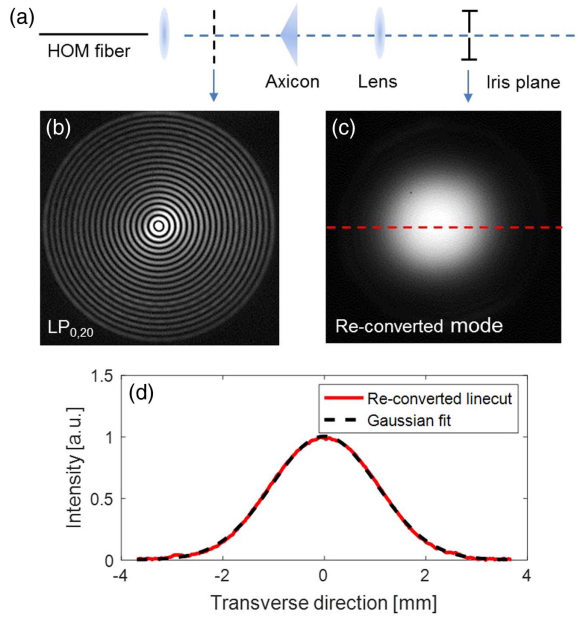

Fig. 4. (a) Experimental setup for mode re-conversion. (b) Image of the $LP_{0,20}$ output mode. (c) Gaussian-like beam re-converted using axicon after spatial filtering. (d) Linecut of re-converted beam and corresponding Gaussian fit indicating the high spatial coherence of modes obtained via SSMC.

The final data point in Fig. 3 represents a 1.1-MW peak power pulse (80 nJ, 74 fs) at 1317 nm; the mode image is shown in Fig. 4(b). The seemingly pure $LP_{0,20}$ mode image suggests that the output is a high-quality spatially coherent, and *single-mode* beam. We investigate the mode quality via axicon-lens-based conversion of the output beam into a Gaussian-shaped beam, using the experimental setup shown in Fig. 4(a). This schematic should yield a perfect Gaussian with a theoretical transmission of 86% if the output is indeed a single-mode beam with a well-controlled spatial phase [26]. The fact that we obtain a high-quality Gaussian beam [image in Fig. 4(c), fit in Fig. 4(d)] with a measured transmission of 81%—close to theoretical prediction—combined with the fact that the pulse is transform limited, indicates that SSMC yields spatiotemporally coherent pulses. This SSMC output may be used as is, since it resembles a truncated Bessel beam [27], which has found several beneficial applications in microscopy [28], or may be converted into a conventional Gaussian beam with minimal loss.

4. DISCUSSION, SUMMARY, AND CONCLUSION

The SSMC effect we have described here is a nonlinear scattering mechanism that fully converts an ultrashort soliton in one spatial mode into a group-velocity-matched soliton in a distinct spatial mode. The driving mechanism is the existence of substantial Raman gain for a noise-initiated pulse that, despite being at large spectral separation from the "pump" pulse, has identical group velocity as well as anomalous GVD. The interesting observation is that a system comprising more than 10,000 spatial modes self-selects precisely one nonlinear process and facilitates full photon conversion. In doing so, this noise-initiated process even subsumes the competing nonlinearity of self-seeded Raman soliton shifting (SSFS) that is ubiquitous for intense ultrashort pulses in anomalous GVD fibers. In contrast, most other nonlinear coupling phenomena become dominant and offer full pump depletion or complete conversion only when the process is externally seeded, as with parametric converters [29], self-seeded, as with SSFS [1] and self-focusing [30], constrained by filtering, either spectrally as with similariton fiber lasers [31,32] or temporally as with passive mode locking using a saturable absorber [33], or operated in a resonant cavity, as with parametric oscillators [34]. Even so, the nonlinearly generated wave often acts as a secondary pump for cascaded nonlinear effects, hence limiting full conversion. Thus, SSMC is a manifestation of Raman scattering that has no direct analogs to known nonlinear effects in bulk media or single-mode waveguides.

We used step-index multimode fibers for our experiments because they possess several attributes that are attractive for this and many other nonlinear optical applications. It is well known that the spacing of propagation constants or group-velocity is irregular in step-index fibers, which means that spectral separations at which the group velocities are matched between modes change with mode order. This explains the exclusive coupling between only two modes in a fiber with a multitude of modes. In addition, light propagation stability in step-index fibers increases with radial order for zero-angular-momentum modes (the so-called $LP_{0,m}$; $m \in$ radial order) [19]—this helps maintain spatial coherence of the nonlinear products. Finally, modes in step-index fibers possess anomalous GVD [20] and large mode areas [35].

Hence, step-index fibers yield a power-scalable platform in which GVD and intermodal group-velocity can be tailored by mode choice and fiber core size. Using SSMC, we demonstrate ~600-nm wavelength translations starting from 1045 nm, as well as the ability to obtain record peak powers (>1 MW) at the biologically crucial ~1300-nm wavelength range [36]. This represents an enhancement, by roughly two orders of magnitude, in the frequency-converted power obtained directly out of any flexible fiber to date. More generally, given that the requirements are simply a multimode waveguide with irregular group-velocity spacings (thus, any multimode waveguide except for the special case of parabolic index profile, graded index fibers, where group velocities of all modes are, by design, nearly identical), we expect that this work can be extended to several other wavelengths (e.g., visible or mid-IR) as well as platforms (e.g., on-chip waveguides) as a generalized scheme for nonlinear ultrafast frequency conversion in a power-scalable fashion. Thus, SSMC bridges the gap between conventional waveguide nonlinear optics, which facilitates diverse wavelength conversion in an integrated format, but with power limitations, and parametric oscillators/amplifiers, which are power scalable but in bulk, alignment-sensitive formats.

Funding. Air Force Office of Scientific Research (AFOSR) (FA9550-14-1-0165); Office of Naval Research (ONR) (N00014-17-1-2519); Det Frie Forskningsråd (DFF) (DFF—1337-00150); National Institutes of Health (NIH) (1R21EY026410-01).

Acknowledgment. The authors would like to thank G. P. Agrawal and A. Antikainen for insightful discussions. The authors acknowledge KMLabs for use of its ultrafast ytterbium-doped fiber pump laser, and cooperation in the attendant optimization of the laser for the experiments.

See Supplement 1 for supporting content.

REFERENCES

1. F. M. Mitschke and L. F. Mollenauer, "Discovery of the soliton self-frequency shift," Opt. Lett. **11**, 659–661 (1986).
2. R. H. Stolen, E. P. Ippen, and A. R. Tynes, "Raman oscillation in glass optical waveguide," Appl. Phys. Lett. **20**, 62–64 (1972).
3. K. S. Chiang, "Stimulated Raman scattering in a multimode optical fiber: evolution of modes in Stokes waves," Opt. Lett. **17**, 352–354 (1992).
4. H. Pourbeyram, G. P. Agrawal, and A. Mafi, "Stimulated Raman scattering cascade spanning the wavelength range of 523 to 1750 nm using a graded-index multimode optical fiber," Appl. Phys. Lett. **102**, 201107 (2013).
5. M. Ziemienczuk, A. M. Walser, A. Abdolvand, and P. St. J. Russell, "Intermodal stimulated Raman scattering in hydrogen-filled hollow-core photonic crystal fiber," J. Opt. Soc. Am. B **29**, 1563–1568 (2012).
6. A. Hasegawa, "Self-confinement of multimode optical pulse in a glass fiber," Opt. Lett. **5**, 416–417 (1980).
7. J. P. Gordon, "Theory of the soliton self-frequency shift," Opt. Lett. **11**, 662–664 (1986).
8. W. H. Renninger and F. W. Wise, "Optical solitons in graded-index multimode fibres," Nat. Commun. **4**, 1719 (2013).
9. L. G. Wright, W. H. Renninger, D. N. Christodoulides, and F. W. Wise, "Spatiotemporal dynamics of multimode optical solitons," Opt. Express **23**, 3492–3506 (2015).
10. L. G. Wright, D. N. Christodoulides, and F. W. Wise, "Controllable spatiotemporal nonlinear effects in multimode fibres," Nat. Photonics **9**, 306–310 (2015).
11. K. Krupa, C. Louot, V. Couderc, M. Fabert, R. Guenard, B. M. Shalaby, A. Tonello, D. Pagnoux, P. Leproux, A. Bendahmane, R. Dupiol, G. Millot, and S. Wabnitz, "Spatiotemporal characterization of supercontinuum extending from the visible to the mid-infrared in a multimode graded-index optical fiber," Opt. Lett. **41**, 5785–5788 (2016).
12. S. W. Hell, "Far-field optical nanoscopy," Science **316**, 1153–1158 (2007).
13. N. Bozinovic, Y. Yue, Y. Ren, M. Tur, P. Kristensen, H. Huang, A. E. Willner, and S. Ramachandran, "Terabit-scale orbital angular momentum mode division multiplexing in fibers," Science **340**, 1545–1548 (2013).
14. A. Antikainen, L. Rishøj, B. Tai, S. Ramachandran, and G. P. Agrawal, "Fate of a soliton in a high order spatial mode of a multimode fiber," Phys. Rev. Lett. **122**, 023901 (2019).
15. L. Rishoj, B. Tai, P. Kristensen, and S. Ramachandran, "High power spatially coherent pulse formation via intermodal soliton interactions in fiber," in *Advanced solid-state lasers (ASSL)* (2016), paper ATh1A.6.
16. C. R. Menyuk, "Stability of solitons in birefringent optical fibers. I: Equal propagation amplitudes," Opt. Lett. **12**, 614–616 (1987).
17. N. Nishizawa and G. Toshio, "Trapped pulse generation by femtosecond soliton pulse in birefringent optical fibers," Opt. Express **10**, 256–261 (2002).
18. Q. F. Yang, X. Yi, K. Y. Yang, and K. Vahala, "Stokes solitons in optical microcavities," Nat. Phys. **13**, 53–57 (2016).
19. S. Ramachandran, J. W. Nicholson, S. Ghalmi, M. F. Yan, P. Wisk, E. Monberg, and F. V. Dimarcello, "Light propagation with ultralarge modal areas in optical fibers," Opt. Lett. **31**, 1797–1799 (2006).
20. S. Ramachandran, J. M. Fini, M. Mermelstein, J. W. Nicholson, S. Ghalmi, and M. F. Yan, "Ultra-large effective-area, higher-order mode fibers: a new strategy for high-power lasers," Laser Photon. Rev. **2**, 429–448 (2008).
21. X. Liu, C. Xu, W. H. Knox, J. K. Chandalia, B. J. Eggleton, S. G. Kosinski, and R. S. Windeler, "Soliton self-frequency shift in a short tapered air-silica microstructure fiber," Opt. Lett. **26**, 358–360 (2001).
22. L. Rishoj, G. Prabhakar, J. Demas, and S. Ramachandran, "30 nJ, ~50 fs all-fiber source at 1300 nm using soliton shifting in LMA HOM fiber," in *Conference on Lasers and Electro-Optics (CLEO)* (2016), paper STh3O.3.
23. B. Tai, L. Rishøj, and S. Ramachandran, "Ultrafast, high energy, wideband wavelength conversion via continuous intra-pulse and discrete intermodal Raman scattering," in *Conference on Lasers and Electro-Optics (CLEO)* (2018), paper SM1K.1.
24. L. Rishoj, B. Tai, P. Kristensen, and S. Ramachandran, "Characterization of intermodal group index matched soliton interactions leading to MW peak powers at 1300 nm," in *Conference on Lasers and Electro-Optics (CLEO)* (2017), paper STh3K.2.
25. A. Antikainen, B. Tai, L. Rishøj, S. Ramachandran, and G. P. Agrawal, "Intermodal Raman scattering of ultrashort pulses in multimode fibers," in *Conference on Lasers and Electro-Optics (CLEO)* (2018), paper FTh4E.3.
26. J. Demas, L. Rishøj, and S. Ramachandran, "Free-space beam shaping for precise control and conversion of modes in optical fiber," Opt. Express **23**, 28531–28545 (2015).
27. P. Steinvurzel, K. Tantiwanichapan, M. Goto, and S. Ramachandran, "Fiber-based Bessel beams with controllable diffraction-resistant distance," Opt. Lett. **36**, 4671–4673 (2011).
28. F. O. Fahrbach, P. Simon, and A. Rohrbach, "Microscopy with self-reconstructing beams," Nat. Photonics **4**, 780–785 (2010).
29. S. A. Akhmanov, A. I. Kovrigin, A. S. Piskarskas, V. V. Fadeev, and R. V. Khokhlov, "Observation of parametric amplification in the optical range," J. Exp. Theor. Phys. **2**, 191–193 (1965).
30. R. Y. Chiao, E. Garmire, and C. H. Townes, "Self-trapping of optical beams," Phys. Rev. Lett. **13**, 479–482 (1964).
31. M. E. Fermann, V. I. Kruglov, B. C. Thomsen, J. M. Dudley, and J. D. Harvey, "Self-similar propagation and amplification of parabolic pulses in optical fibers," Phys. Rev. Lett. **84**, 6010–6013 (2000).
32. A. Chong, J. Buckley, W. Renninger, and F. Wise, "All-normal-dispersion femtosecond fiber laser," Opt. Express **14**, 10095–10100 (2006).
33. A. J. DeMaria, D. A. Stetser, and H. Heynau, "Self mode-locking of lasers with saturable absorbers," Appl. Phys. Lett. **8**, 174–176 (1966).
34. J. A. Giordmaine and R. C. Miller, "Tunable coherent parametric oscillation in $LiNbO_3$ at optical frequencies," Phys. Rev. Lett. **14**, 973–976 (1965).
35. J. W. Nicholson, J. M. Fini, A. M. DeSantolo, X. Liu, K. Feder, P. S. Westbrook, V. R. Supradeepa, E. Monberg, F. DiMarcello, R. Ortiz, C. Headley, and D. J. DiGiovanni, "Scaling the effective area of higher-order-mode erbium-doped fiber amplifiers," Opt. Express **20**, 24575–24584 (2012).
36. N. G. Horton, K. Wang, D. Kobat, C. G. Clark, F. W. Wise, C. B. Schaffer, and C. Xu, "In vivo three-photon microscopy of subcortical structures within an intact mouse brain," Nat. Photonics **7**, 205–209 (2013).